Structural and Magnetic Properties of a Drop-Cast C 54 H 34 Br 4 CuO 4 β-Diketonato Complex Film on a Graphite Surface

Emilio Vélez-Fort, Philippe Ohresser, Mathieu Silly, Jacques Bonvoisin, Fabien Silly

Structural and Magnetic Properties of a Drop-Cast $C_{54}H_{34}Br_4CuO_4$ β-Diketonato Complexes Film on a Graphite Surface at 2 K

Emilio Vélez-Fort,[†] Philippe Ohresser,[*,‡] Mathieu G. Silly,[‡] Jacques Bonvoisin,[*,¶] and Fabien Silly[*,§]

†*European Synchrotron Radiation Facility (ESRF), Avenue des Martyrs 71, 38043 Grenoble, France*

‡*Synchrotron SOLEIL, L'Orme des Merisiers, F-91190 Saint-Aubin, France*

¶*CEMES, CNRS UPR 8011, Université de Toulouse, 29 rue Jeanne Marvig, B.P. 94347, 31055 Toulouse Cedex 4, France*

§*Université Paris-Saclay, CEA, CNRS, SPEC, TITANS F-91191 Gif sur Yvette, France*

E-mail: philippe.ohresser@synchrotron-soleil.fr; jacques.bonvoisin@cemes.fr; fabien.silly@cea.fr,Tel:+33(0)169088019,Fax:+33(0)169088446

Abstract

The structural and magnetic properties of a drop-cast film of flat $C_{54}H_{34}Br_4CuO_4$, a β-diketonato complex functionalized with bromine atoms, on a graphite surface are investigated using scanning tunneling microscopy and synchrotron X-ray absorption spectroscopy and X-ray magnetic circular dichroism. Experimental measurements reveal that the Cu-complexes preferentially lay flat on the graphite surface. The magnetic hysteresis loops show that the

organic thin film remains paramagnetic at 2 K with an easy axis of magnetization perpendicular to the graphite surface and is therefore perpendicular to the plane of the Cu-complex skeleton.

Introduction

Magnetism in two-dimensional (2D) materials is the focus of recent research interest due to the exciting properties emerging at nanoscale and and the potential of these materials for applications ranging from spintronics, quantum computing to optical communications.[1–4] Magnetic 2D organic materials can be engineered taking advantage of the self-assembly of molecular magnets. The magnetic properties of such 2D materials are expected to not only depend of the intrinsic magnetic properties of the individual building blocks but also their arrangement. Controlling the properties of self-assembled magnetic nanoarchitecture requires a precise assessment of self-assembly processes as well as a detailed characterization of the material structure combined with proper magnetic properties characterization.

Selective and directional intermolecular interactions allow controlling molecular assembly into specific arrangements. Large scale 2D self-assembled organic nanoarchitectures stabilised by hydrogen-bonds have thus been achieved.[5–21] In contrast self-assembled halogen-bonded 2D organic structures have only been recently investigated.[22–46]

In this paper we synthesise a flat β-diketonato copper complex with bromine substituent to trigger the formation of magnetic organic 2D material stabilized by halogen-bonds on a graphite surface. Molecular self-assembly is investigated using scanning tunneling microscopy and XNLD (X-ray Natural Linear Dichroism). The magnetic properties of the organic layer is assessed using the high sensitivity of XMCD (X-ray Magnetic Circular Dichroism).

Experimental

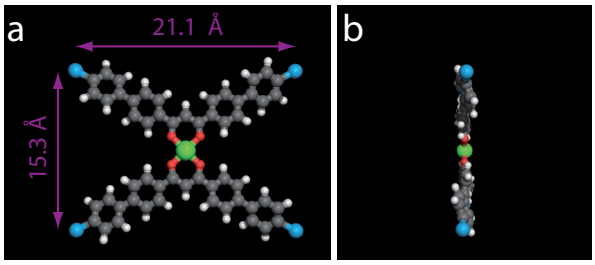

Figure 1: Scheme of the β-diketonato copper complex, $C_{54}H_{34}Br_4CuO_4$ in square-planar complex [Cu(II)(*bbbpd*)$_2$]^0 conformation in front and side views (a,b). Carbon atoms are gray, bromine atoms are light blue, hydrogen atoms are white, oxygen atoms are red and copper atom is green, respectively.

The chemical structure of the β-diketonato copper complex (Cu(II)(*bbbpd*)$_2$) is presented in Figure 1. This 2-fold symmetry complex is a H-shaped complex. The closest coordination environment of the copper atom is formed by four oxygen atomes belonging to two acetylacetonate type ligands. Bromine atoms are located at the apex of the four complex arms. The Bromine atom separations are 21.1 Å and 15.3 Å.

Solutions of the complexes in *1*-phenyloctane (Aldrich) were prepared. A droplet of the solutions was then deposited on a graphite substrate. STM imaging of the samples was performed at the liquid-solid interface using a Pico-SPM (Molecular Imaging, Agilent Technology) scanning tunneling microscope. Cut Pt/Ir tips were used to obtain constant current images at room temperature with a bias voltage applied to the sample. Scanning Tunneling Microscopy (STM) images were processed and analyzed using the application FabViewer.[47]

The chemical selected magnetization loops, the XMCD and the XNLD have been measured on the DEIMOS beamline at SOLEIL Synchrotron.[48,49] All the X-ray Absorption Spectroscopy (XAS) measurement presented in this paper have been performed at a low temperature of 2 K in a cryomagnet with a base pressure of 1.10^{-10} mbar. The photon flux has been reduced at the low-

est (typically 6.10^9 ph/s) to avoid any possible beam damage. The typical edge jumps are around few percent of the background and to obtain a good statistic a typical dichroism measurement (XMCD or XNLD) is obtained by taking thirty two XAS spectra recorded with opposite orientation of the magnetic field (for the case of XMCD) and flipping the helicity of the light. XAS has been measured for horizontal and vertical linear polarizations at grazing incidence to determine the adsorption geometry of the molecules on the surface. The XMCD spectrum corresponds to the difference of the XAS spectra measured with left and right helicity of the light while XNLD is obtained using vertical and horizontal linear polarized light. For the sake of simplicity, we will call μ^+, μ^-, μ^H and μ^V the absorption coefficient of respectively left-, right-circular, horizontal and vertical linear polarized light.

Results

Scanning Tunneling Microscopy (STM)

The STM image in Figure 2 shows the graphite surface after deposition of a droplet of the Cu-complex in *1*-phenyloctane. Molecules self-assemble into a large-scale 2D organic porous nanoarchitecture at the interface with the graphite surface. The organic network is composed of parallel rows of molecules. Neighboring rows are shifted along their axis by half a complex-length. The model of the molecular arrangement is superimposed to the experimental STM image in Figure 2. The network unit, containing one molecule, is represented by dashed purple lines. The unit cell of this porous structure is a parallelogram with 2.5 ± 0.1 nm and 2.6 ± 0.1 nm unit cell constants

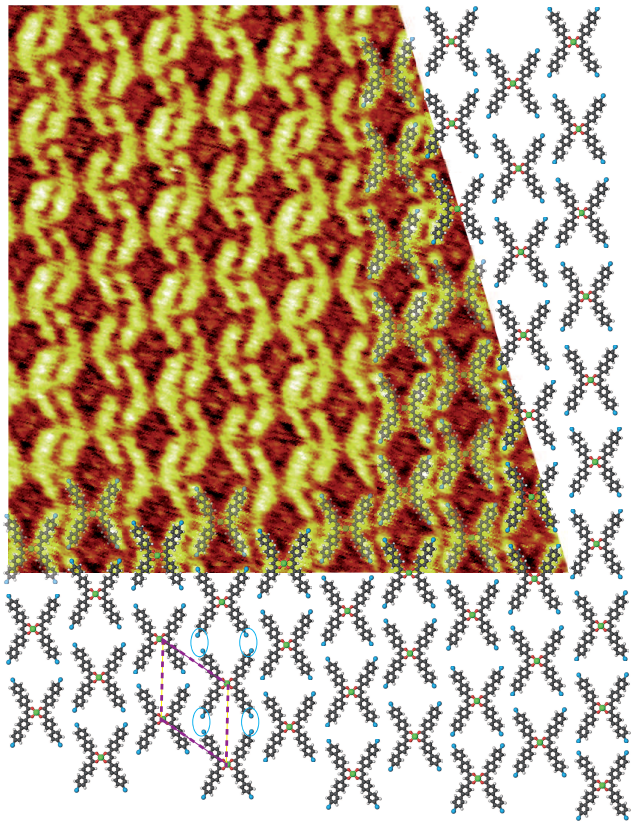

Figure 2: STM image of the Cu-complex self-assembled porous network at the **1**-phenyloctane/graphite interface, (a) 17×17 nm^2, V_s = 0.95 V, I_t = 9 pA. Model of the molecular assembly is superimposed to the STM image. The parallelogram unit cell is represented by dashed-purple lines.

and an angle of $55 \pm 1^{\circ}$ between the axes.

The complex arrangement is stabilized by Br$\cdots$Br interactions along the molecular rows. These halogen-bonds are highlighted by blue ellipses in Figure 2. No halogen interactions are observed between molecules of neighboring rows. The arms of the molecules in neighboring rows are arranged side-by-side, which is favoring van der Waals interactions.

X-ray Natural Linear Dichroism (XNLD)

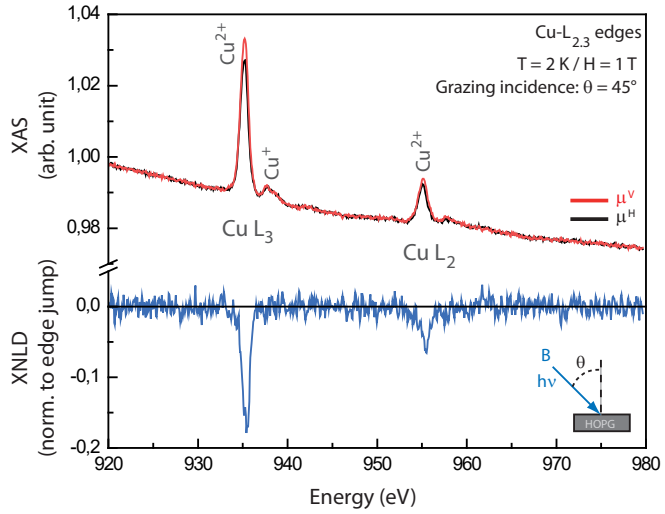

Figure 3: Experimental XAS (black and black curves, top) and XNLD (blue curve, bottom) spectra of the copper β-Diketonato complex film on HOPG, recorded for the Cu $L_{2,3}$ edges at temperature of 2 K, an applied external magnetic field of 1 T and an incidence angle of 45 °. The XNLD spectra (μ^V - μ^H) have been normalized to the L_3 edge jump of the corresponding XAS spectra ((μ^V + μ^H)/2)

The sample is then introduced into the UHV chamber, achieving solvent evaporation in order to perform XAS measurements. The orientation of the molecules adsorbed on the surface is now investigated using XAS spectroscopy,[50,51] Figure 3. The electronic anisotropy of the sample structure at a temperature of 2 K is assessed by linear polarization at a grazing incidence of θ = 45 °, Figure 3. The μ^V and μ^H polarizations are probing the in-plane and out-of plane electronic configuration, respectively. The XNLD curve in blue corresponds to the difference between the μ^H - μ^V spectra.

Several peaks are observed in the XAS spectra, Figure 3,top. Kuterasinski*et al.* showed that the copper oxidation state (Cu^+ and Cu^{2+}) of Cu-complexes are revealed by the XAS spectroscopy.[52] Comparison of the peaks in Figure 3 with those observed in the litterature displays that the main peaks observed in Figure 3 at the Cu-$L_{2,3}$ edges (red and black curves for μ^H and μ^V polarisations)

corresponds to the signature of the Cu^{2+} species. The smaller contribution visible at higher energy corresponds to the Cu^{+} lower oxidation state.[52–54] The XAS spectra in Figure 3,top establishes that the presence of Cu^{+} species is drastically smaller than the one of the Cu^{2+} species.

An XNLD signal is observed for the $L_{2,3}$ edges of Cu^{2+} but not for the Cu^{+} contribution. This observation first confirms that planar conformation of the Cu^{2+} β-Diketonato complexes (Figure 1) on HOPG, as observed by STM (Figure 2). The flat Cu^{2+} β-diketonato copper complex possesses in it center a Cu^{2+} ion with in-plane $d_{x^2-y^2}$ orbitals. As the dichroism in the XAS spectra is maximal for the electric field (E) parallel the surface plane and minimal for E oriented out of plane, this indicated that the complex planar skeleton preferentially lies parallel to the plane of the HOPG surface.

No XNLD signal is observed for Cu^{+} β-Diketonato complexes. This observation confirms that the Cu^{+} complexes have a non-planar molecular conformation, as previously observed.[55]

X-ray Magnetic Circular Dichroism (XMCD)

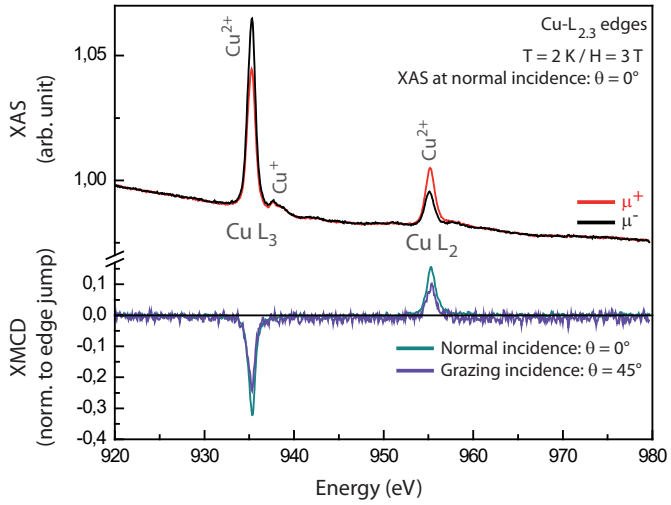

Figure 4: (top) Polarization dependent XAS spectra of the Cu-complexes on HOPG recorded at the Cu $L_{2,3}$ edges at normal (θ = 0 °) incidence (right) as a function of circular polarization (μ^+, red spectrum, and μ^-, black spectrum). (Bottom) XMCD spectra (μ^+,μ^-) derived from the XAS spectra recorded at normal (θ = 0 °, green spectrum) and grazing (θ = 45 °, purple spectrum) incidences. The XMCD spectra have been normalized to the L_3 edge jump of the corresponding XAS spectra ((μ^++ μ^-)/2). The All the measurements have been performed at a temperature of 2 K, an applied external magnetic field B = 3 T

The magnetic properties of the Cu-complex thin film on HOPG are now investigated using XAS with circularly polarized light to determine the XMCD signal, Figure 4,top. The XAS spectra at the Cu $L_{2,3}$ edges are recorded at the normal (θ = 0 °) and grazing (θ = 45 °) and a temperature of 2 K and under a magnetic field B = 3 T. Significant circular dichroism is visible in the XAS spectra for the Cu^{2+} state of the Cu-complex, Figure 4,bottom. This indicates that the organic film has a non-zero magnetization under an applied field of 3 T. The resulting XMCD spectra (difference between the absorption of μ^- and μ^+ circular polarized light), recorded at normal incidence (θ = 0 °) and grazing incidence (θ = 45 °) show a larger contribution for the normal geometry , with a value of $\sim$30% at the Cu-L_3 edge at normal incidence and 25% at the θ = 45 ° grazing incidence.

Magnetization Curves

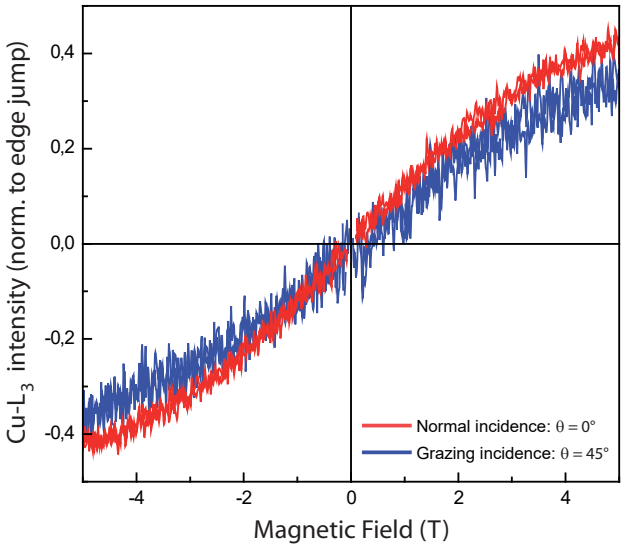

Figure 5: Magnetic hysteresis loops measured at 2 K on the copper β-Diketonato complex film on HOPG at the normal incidence (θ = 0 °, red curve) and the grazing incidence (θ = 45 °, blue curve). The measurements have been normalized in intensity to the corresponding XMCD signal (see Figure 4.)

Figure 5 shows the magnetization curves of the Copper β-Diketonato complex film on HOPG at a normal incidence ($\theta = 0\,^{\circ}$) and at a grazing incidence ($\theta = 45\,^{\circ}$) at 2 K. These curves are obtained by recording the variation of the maximum Cu-L_3 XMCD intensity with the applied magnetic field.

Figure 5 reveals that the magnetization curves are not saturated at 2 K for 5 T with a paramagnetic shape for both geometries. This shows that the molecular film has a paramagnetic behaviour with a small anisotropy favouring out-of-plane geometry.

Discussion

A solution of β-Diketonato complexes with bromine substituents (Figure 1) has been deposited onto a HOPG surface. STM at the solid-liquid interface reveals that the molecules self-assembled into a porous nanoarchitecture stabilized by halogen-bonds and van der Waals interactions, Figure 2. The molecules adsorb flat on the HOPG surface. This local STM observation is further confirm at a macroscopic scale by XNLD, after The sample is then transferred to the UHV chamber.

A signal of $\sim$20% is observed in the XNLD spectrum at the Cu-L_3 edge at grazing incidence. This shows that the molecules laying parallel to the plane of the HOPG surface. The central Cu^{2+} ion surrounded by for oxygen atom in the flat β-Diketonato skeleton has an in-plane $d_{x^2y^2}$ orbital geometry. The Cu^{2+} ion surrounded by four nitrogen atoms in the square-planar phthalocyanine skeleton also has $d_{x^2y^2}$ electronic structure.[50] For such compound, the XNLD signal at θ = 70 ° reaches $\sim$90%, when isolated Cu^{2+}-phthalocyanines are lying flat on Ag(111).[56] The different geometry (θ = 45 ° use in Figure 3 leads to smaller XNLD but it can be estimated that the drop cast film of β-Diketonato complexes is nevertheless roughly two time more disordered than nearly defect-free isolated Cu-phthalocyanines molecules. The drop-cast β-Diketonato complex film cannot be considered as a homogeneous material composed multilayers of parallel molecules, but the flat molecular orientation is in average well preserved.

A stronger XMCD signal is observed at normal incidence. This shows that the magnetic anisotropy of the Cu^{2+}-complex thin film has an easy axis of magnetization perpendicular to the HOPG surface. The magnetic anisotropy is therefore perpendicular to the plane of the Cu^{2+}-complex skeleton. The magnetisation curves of the Cu-complex thin film also reveal that the

organic film on HOPG remains paramagnetic at 2 K. Lower temperatures are required to observe possible ferromagnetism in the organic layer.

A small amount of Cu^{+}-complexes is detected by the X-ray spectroscopy. Magnetic measurements reveals that this species is non-magnetic, in constrast with the Cu^{2+} species.

Conclusion

To summarize, we have engineered a drop-cast film of flat β-diketonato complexes on a non-magnetic graphite surface. Scanning tunneling microscopy and synchrotron radiation spectroscopies show that the molecules are forming halogen-bonds and are preferentially laying flat on the graphite surface. The organic Cu^{2+}-complex thin film remains paramagnetic at 2 K, but its the magnetic anisotropy appears to have an easy axis of magnetization perpendicular to the molecular plane. These observations open up new opportunities for engineering magnetic halogen-bonded nanoarchitectures through drop-casting. Optimizing the film structure and modifying molecular arrangement, by the wise selection of molecular halogen substituents, is expected to improve the magnetic properties of the organic film.

Acknowledgement

The research leading to these results has received funding from the European Research Council under the European Union's Seventh Framework Programme (FP7/2007-2013) / ERC grant agreement n ° 259297. Experiments were performed on the DEIMOS beamline at SOLEIL Synchrotron, France (proposal number 20220737). We are grateful to the SOLEIL staff for smoothly running

the facility.

Author informations:

Emilio Vélez-Fort: 0000-0002-0362-0366

Philippe Ohresser: 0000-0001-8611-1753

Mathieu Silly: 0000-0002-0302-8442

Jacques Bonvoisin: 0000-0003-3741-9529

Fabien Silly: 0000-0001-6782-9268

References

1. Elahi, E.; Dastgeer, G.; Nazir, G.; Nisar, S.; Bashir, M.; Akhter Qureshi, H.; Kim, D.-k.; Aziz, J.; Aslam, M.; Hussain, K.; Assiri, M. A.; Imran, M. A review on Two-Dimensional (2D) Magnetic Materials and their Potential Applications in Spintronics and Spin-Caloritronic. *Comput. Mater. Sci.* **2022**, *213*, 111670.

2. Wang, Q. H.; Bedoya-Pinto, A.; Blei, M.; Dismukes, A. H.; Hamo, A.; Jenkins, S.; Koperski, M.; Liu, Y.; Sun, Q.-C.; Telford, E. J.; Kim, H. H.; Augustin, M.; Vool, U.; Yin, J.-X.; Li, L. H.; Falin, A.; Dean, C. R.; Casanova, F.; Evans, R. F. L.; Chshiev, M. *et al.* The Magnetic Genome of Two-Dimensional van der Waals Materials. *ACS Nano* **2022**, *16*, 6960–7079.

3. Jiang, X.; Liu, Q.; Xing, J.; Liu, N.; Guo, Y.; Liu, Z.; Zhao, J. Recent Progress on 2D Magnets: Fundamental Mechanism, Structural Design and Modification. *Appl. Phys. Rev. 8*, 031305.

4. López-Cabrelles, J.; Manas-Valero, S.; Vitórica-Yrezábal, I. J.; Siskins, M.; Lee, M.; Steeneken, P. G.; Zant, H. S. J. v. d.; Espallargas, G. M.; Coronado, E. Chemical Design and Magnetic Ordering in Thin Layers of 2D Metal–Organic Frameworks (MOFs). *J. Am. Chem. Soc.* **2021**,

5. Yagai, S. Supramolecularly Engineered Functional π-Assemblies Based on Complementary Hydrogen-Bonding Interactions. *Bull. Chem. Soc. Jpn* **2015**, *88*, 28–58.

6. Xu, L.; Miao, X.; Zha, B.; Deng, W. Hydrogen-Bonding-Induced Polymorphous Phase Transitions in 2D Organic Nanostructures. *Chem. - An Asian J.* **2013**, *8*, 926–933.

7. Tanioku, C.; Matsukawa, K.; Matsumoto, A. Thermochromism and Structural Change in Polydiacetylenes Including Carboxy and 4-Carboxyphenyl Groups as the Intermolecular Hydrogen Bond Linkages in the Side Chain. *ACS Appl. Mater. Inter.* **2013**, *5*, 940–948.

8. Hu, Y.; Miao, K.; Zha, B.; Xu, L.; Miao, X.; Deng, W. STM Investigation of Structural Isomers: Alkyl Chain Position Induced Self-Assembly at the Liquid/Solid Interface. *Phys. Chem. Chem. Phys.* **2015**, *18*, 624–634.

9. Priimagi, A.; Lindfors, K.; Kaivola, M.; Rochon, P. Efficient Surface-Relief Gratings in Hydrogen-Bonded Polymer-Azobenzene Complexes. *ACS Appl. Mater. Inter.* **2009**, *1*, 1183–1189.

10. Hu, Y.; Miao, K.; Peng, S.; Zha, B.; Xu, L.; Miao, X.; Deng, W. Structural Transition Control Between Dipole–Dipole and Hydrogen Bonds Induced Chirality and Achirality. *CrystEngComm* **2016**, *18*, 3019–3032.

11. Hieulle, J.; Silly, F. Localized Intermolecular Electronic Coupling in Two-Dimensional Self-Assembled 3,4,9,10-perylenetetracarboxylic Diimide Nanoarchitectures. *J. Mater. Chem. C* **2013**, *1*, 4536–4539.

12. Barth, J. V. Molecular Architectonic on Metal Surfaces. *Annu. Rev. Phys. Chem.* **2007**, *58*, 375–407.

13. Uemura, S.; Aono, M.; Komatsu, T.; Kunitake, M. Two-Dimensional Self-Assembled Structures of Melamine and Melem at the Aqueous Solution-Au(111) Interface. *Langmuir* **2011**, *27*, 1336–1340.

14. Silly, F. Two-Dimensional 1,3,5-Tris(4-carboxyphenyl)benzene Self-Assembly at the 1-Phenyloctane/Graphite Interface Revisited. *J. Phys. Chem. C* **2012**, *116*, 10029–10032.

15. Shen, C.; Cebula, I.; Brown, C.; Zhao, J.; Zharnikov, M.; Buck, M. Structure of Isophthalic Acid Based Monolayers and its Relation to the Initial Stages of Growth of Metal-Organic Coordination Layers. *Chem. Sci.* **2012**, *3*, 1858–1865.

16. Temirov, R.; Soubatch, S.; Neucheva, O.; Lassise, A. C.; Tautz, F. S. A Novel Method Achieving Ultra-High Geometrical Resolution in Scanning Tunnelling Microscopy. *New J. Phys.* **2008**, *10*, 053012.

17. Chen, T.; Yang, W.-H.; Wang, D.; Wan, L.-J. Globally Homochiral Assembly of Two-Dimensional Molecular Networks Triggered by Co-Absorbers. *Nat. Commun.* **2013**, *4*, 1389.

18. Liang, H.; Sun, W.; Jin, X.; Li, H.; Li, J.; Hu, X.; Teo, B. K.; Wu, K. Two-Dimensional Molecular Porous Networks Formed by Trimesic Acid and 4,4'Bis(4-pyridyl)biphenyl on Au(111)

through Hierarchical Hydrogen Bonds: Structural Systematics and Control of Nanopore Size and Shape. *Angew. Chem., Int. Ed.* **2011**, *50*, 7562–7566.

19. Gardener, J. A.; Shvarova, O. Y.; Briggs, G. A. D.; Castell, M. R. Intricate Hydrogen-Bonded Networks: Binary and Ternary Combinations of Uracil, PTCDI, and Melamine. *J. Phys. Chem. C* **2010**, *114*, 5859–5866.

20. Sun, X.; Jonkman, H. T.; Silly, F. Tailoring Two-Dimensional PTCDA-melamine Self-Assembled Architectures at Room Temperature by Tuning Molecular Ratio. *Nanotech.* **2010**, *21*, 165602.

21. Räisänen, M. T.; Slater, A. G.; Champness, N. R.; Buck, M. Effects of Pore Modification on the Templating of Guest Molecules in a 2D Honeycomb Network. *Chem. Sci.* **2011**, *3*, 84–92.

22. Wang, Y.; Zou, H.; Liu, Y.; Miao, X.; Deng, W.; Yuan, Q. FBr and F$\cdots$S Heterohalogen-Bond-Directed 2D Self-Assemblies of a Benzothiadiazole Derivative. *Langmuir* **2023**,

23. Shang, J.; Wang, Y.; Chen, M.; Dai, J.; Zhou, X.; Kuttner, J.; Hilt, G.; Shao, X.; Gottfried, J. M.; Wu, K. Assembling Molecular Sierpiński Triangle Fractals. *Nat. Chem.* **2015**, *7*, 389–393.

24. Xu, J.; Liu, X.; Ng, J. K.-P.; Lin, T.; He, C. Trimeric Supramolecular Liquid Crystals Induced by Halogen Bonds. *J. Mater. Chem.* **2006**, *16*, 3540–3545.

25. Gao, H. Y.; Shen, Q. J.; Zhao, X. R.; Yan, X. Q.; Pang, X.; Jin, W. J. Phosphorescent Co-Crystal Assembled by 1,4-diiodotetrafluorobenzene with Carbazole Based on C-I$\cdots\pi$ Halogen Bonding. *J. Mater. Chem.* **2012**, *22*, 5336–5343.

26. Silly, F. Selecting Two-Dimensional Halogen-Halogen Bonded Self-Assembled 1,3,5-Tris(4-iodophenyl)benzene Porous Nanoarchitectures at the Solid-Liquid Interface. *J. Phys. Chem. C* **2013**, *117*, 20244–20249.

27. Getmanenko, Y. A.; Fonari, M.; Risko, C.; Sandhu, B.; Galán, E.; Zhu, L.; Tongwa, P.; Hwang, D. K.; Singh, S.; Wang, H.; Tiwari, S. P.; Loo, Y.-L.; Brédas, J.-L.; Kippelen, B.; Timofeeva, T.; Marder, S. R. Benzo[1,2-b:6,5-b']dithiophene(dithiazole)-4,5-dione Derivatives: Synthesis, Electronic Properties, Crystal Packing and Charge Transport. *J. Mater. Chem. C* **2013**, *1*, 1467–1481.

28. Metrangolo, P.; Resnati, G.; Pilati, T.; Liantonio, R.; Meyer, F. Engineering Functional Materials by Halogen Bonding. *J. Polym. Sci. Pol. Chem.* **2007**, *45*, 1–15.

29. Meyer, F.; Dubois, P. Halogen Bonding at Work: Recent Applications in Synthetic Chemistry and Materials Science. *CrystEngComm* **2013**, *15*, 3058–3071.

30. Voth, A. R.; Khuu, P.; Oishi, K.; Ho, P. S. Halogen Bonds as Orthogonal Molecular Interactions to Hydrogen Bonds. *Nat. Chem.* **2009**, *1*, 74–79.

31. Lieberman, H. F.; Davey, R. J.; Newsham, D. M. T. Br$\cdots$Br and Br$\cdots$H Interactions in Action: Polymorphism, Hopping, and Twinning in 1,2,4,5-Tetrabromobenzene. *Chem. Mater.* **2000**, *12*, 490–494.

32. Gutzler, R.; Fu, C.; Dadvand, A.; Hua, Y.; MacLeod, J. M.; Rosei, F.; Perepichka, D. F. Halogen Bonds in 2D Supramolecular Self-Assembly of Organic Semiconductors. *Nanoscale* **2012**, *4*, 5965–5971.

33. DiLullo, A.; Chang, S.-H.; Baadji, N.; Clark, K.; Klöckner, J.-P.; Prosenc, M.-H.; Sanvito, S.; Wiesendanger, R.; Hoffmann, G.; Hla, S.-W. Molecular Kondo Chain. *Nano Lett.* **2012**, *12*, 3174–3179.

34. Chung, K.-H.; Kim, H.; Jang, W. J.; Yoon, J. K.; Kahng, S.-J.; Lee, J.; Han, S. Molecular Multistate Systems Formed in Two-Dimensional Porous Networks on Ag(111). *J. Phys. Chem. C* **2013**, *117*, 302–306.

35. Baris, B.; Luzet, V.; Duverger, E.; Sonnet, P.; Palmino, F.; Chérioux, F. Robust and Open Tailored Supramolecular Networks Controlled by the Template Effect of a Silicon Surface. *Angew. Chem., Int. Ed.* **2011**, *50*, 4094–4098.

36. Meazza, L.; Foster, J. A.; Fucke, K.; Metrangolo, P.; Resnati, G.; Steed, J. W. Halogen-Bonding-Triggered Supramolecular Gel Formation. *Nat. Chem.* **2013**, *5*, 42–47.

37. Sun, A.; Lauher, J. W.; Goroff, N. S. Preparation of Poly(diiododiacetylene), an Ordered Conjugated Polymer of Carbon and Iodine. *Science* **2006**, *312*, 1030–1034.

38. Pigge, F. C.; Vangala, V. R.; Kapadia, P. P.; Swenson, D. C.; Rath, N. P. Hexagonal Crystalline Inclusion Complexes of 4-iodophenoxy Trimesoate. *Chem. Commun.* **2008**, 4726–4728.

39. Metrangolo, P.; Meyer, F.; Pilati, T.; Resnati, G.; Terraneo, G. Mutual Induced Coordination in Halogen-Bonded Anionic Assemblies with (6,3) Cation-Templated Topologies. *Chem. Commun.* **2008**, 1635–1637.

40. Zha, B.; Dong, M.; Miao, X.; Peng, S.; Wu, Y.; Miao, K.; Hu, Y.; Deng, W. Cooperation and Competition Between Halogen Bonding and van der Waals Forces in Supramolecular Engi-

neering at the Aliphatic Hydrocarbon/Graphite Interface: Position and Number of Bromine Group Effects. *Nanoscale* **2016**, *9*, 237–250.

41. Zha, B.; Miao, X.; Liu, P.; Wu, Y.; Deng, W. Concentration Dependent Halogen-Bond Density in the 2D Self-Assembly of a Thienophenanthrene Derivative at the Aliphatic Acid/Graphite Interface. *Chem. Commun.* **2014**, *50*, 9003–9006.

42. Peyrot, D.; Silly, F. On-Surface Synthesis of Two-Dimensional Covalent Organic Structures versus Halogen-Bonded Self-Assembly: Competing Formation of Organic Nanoarchitectures. *ACS Nano* **2016**, *10*, 5490–5498.

43. Anh Pham, T.; Song, F.; Nguyen, M.-T.; Stöhr, M. Self-assembly of Pyrene Derivatives on Au(111): Substituent Effects on Intermolecular Interactions. *Chem. Commun.* **2014**, *50*, 14089–14092.

44. Han, Z.; Czap, G.; Chiang, C.-l.; Xu, C.; Wagner, P. J.; Wei, X.; Zhang, Y.; Wu, R.; Ho, W. Imaging the Halogen Bond in Self-Assembled Halogenbenzenes on Silver. *Science* **2017**, *358*, 206–210.

45. Piquero-Zulaica, I.; Lobo-Checa, J.; Sadeghi, A.; El-Fattah, Z. M. A.; Mitsui, C.; Okamoto, T.; Pawlak, R.; Meier, T.; Arnau, A.; Ortega, J. E.; Takeya, J.; Goedecker, S.; Meyer, E.; Kawai, S. Precise engineering of Quantum Dot Array Coupling Through Their Barrier Widths. *Nature Communications* **2017**, *8*, 787.

46. Jang, W. J.; Chung, K.-H.; Lee, M. W.; Kim, H.; Lee, S.; Kahng, S.-J. Tetragonal Porous Networks Made by Rod-Like Molecules on Au(111) with Halogen Bonds. *Appl. Surf. Sci.* **2014**, *309*, 74–78.

47. Silly, F. A Robust Method For Processing Scanning Probe Microscopy Images and Determining Nanoobject Position and Dimensions. *J. Microsc-Oxford* **2009**, *236*, 211–218.

48. Ohresser, P.; Otero, E.; Choueikani, F.; Chen, K.; Stanescu, S.; Deschamps, F.; Moreno, T.; Polack, F.; Lagarde, B.; Daguerre, J.-P.; Marteau, F.; Scheurer, F.; Joly, L.; Kappler, J.-P.; Muller, B.; Bunau, O.; Sainctavit, P. DEIMOS: A Beamline Dedicated to Dichroism Measurements in the 350–2500 eV Energy Range. *Rev. Sci. Instr.* **2014**, *85*, 013106.

49. Joly, L.; Otero, E.; Choueikani, F.; Marteau, F.; Chapuis, L.; Ohresser, P. Fast Continuous Energy Scan with Dynamic Coupling of the Monochromator and Undulator at the DEIMOS Beamline. *J. Synchr. Rad.* **2014**, *21*, 502–506.

50. Willey, T. M.; Bagge-Hansen, M.; Lee, J. R. I.; Call, R.; Landt, L.; van Buuren, T.; Colesniuc, C.; Monton, C.; Valmianski, I.; Schuller, I. K. Electronic Structure Differences Between H2-, Fe-, Co-, and Cu-phthalocyanine Highly Oriented Thin Films Observed using NEXAFS Spectroscopy. *J. Chem. Phys.* **2013**, *139*, 034701.

51. Baby, A.; Marcaud, G.; Dappe, Y. J.; D'Angelo, M.; Cantin, J.-L.; Silly, M. G.; Fratesi, G. Phthalocyanine Reactivity and Interaction on the 6H-SiC(0001)-(3 $\times$ 3) Surface Investigated by Core-Level Experiments and Simulations. *Phys. Chem. Chem. Phys.* **2022**, *24*, 14937–14946.

52. Kuterasiński, u.; Podobiński, J.; Madej, E.; Smoliło-Utrata, M.; Rutkowska-Zbik, D.; Datka, J. Reduction and Oxidation of Cu Species in Cu-Faujasites Studied by IR Spectroscopy. *Molecules* **2020**, *25*, 4765.

53. Jiang, P.; Prendergast, D.; Borondics, F.; Porsgaard, S.; Giovanetti, L.; Pach, E.; Newberg, J.;

Bluhm, H.; Besenbacher, F.; Salmeron, M. Experimental and Theoretical Investigation of the Electronic Structure of Cu_2O and CuO Thin Films on Cu(110) using X-ray Photoelectron and Absorption Spectroscopy. *J. Chem. Phys.* **2013**, *138*, 024704.

54. Davó-Quiñonero, A.; Bailón-García, E.; López-Rodríguez, S.; Juan-Juan, J.; Lozano-Castelló, D.; García-Melchor, M.; Herrera, F. C.; Pellegrin, E.; Escudero, C.; Bueno-López, A. Insights into the Oxygen Vacancy Filling Mechanism in CuO/CeO_2 Catalysts: A Key Step Toward High Selectivity in Preferential CO Oxidation. *ACS Catal.* **2020**, *10*, 6532–6545.

55. Leoni, T.; Guillermet, O.; Walch, H.; Langlais, V.; Scheuermann, A.; Bonvoisin, J.; Gauthier, S. Controlling the Charge State of a Single Redox Molecular Switch. *Phys. Rev. Lett.* **2011**, *106*, 216103.

56. Stepanow, S.; Mugarza, A.; Ceballos, G.; Moras, P.; Cezar, J. C.; Carbone, C.; Gambardella, P. Giant Spin and Orbital Moment Anisotropies of a Cu-Phthalocyanine Monolayer. *Phys. Rev. B* **2010**, *82*, 014405.

TOC Graphic